

Electronic Supplementary Information for: Chemical reactivity from the vibrational ground-state level. The role of the tunneling path in the tautomerization of urea and derivatives

Irea Mosquera-Lois, David Ferro-Costas, and Antonio
Fernández-Ramos*

Centro Singular de Investigación en Química Biolóxica e
Materiais Moleculares (CIQUS);
Universidade de Santiago de Compostela,
15706, Santiago de Compostela, Spain
E-mail*: qf.ramos@usc.es

Contents

1	The ground-state rate constant	3
2	Ground-state vibrationally adiabatic potential	7
2.1	Dual-level MEP	7
2.2	Quasiharmonic correction for anharmonicity	8
3	Anharmonicity on the reaction coordinate frequency	9
4	Stationary points	16

1 The ground-state rate constant

Canonical variational transition state theory (CVT)^{1,2} accounts for two of the main assumptions of conventional transition state theory (i) recrossing and (ii) quantum effects. In particular, it attenuates the recrossing by selecting the rate constant that minimizes the forward flux towards products along a prescribed path. Usually, this path is the minimum energy path (MEP); generalized transition state thermal rate constants along this path are calculated in a similar way as the one obtained by conventional transition state theory. The CVT thermal rate constant is the minimum of these generalized rate constants, and it is given by

$$k^{\text{CVT}}(T) = \frac{1}{h\beta} \frac{Q^{\text{GT}}[T, s_*^{\text{CVT}}(T)]}{\Phi_{\text{R}}(T)} \exp\{-\beta V_{\text{MEP}}[s_*^{\text{CVT}}(T)]\} \quad (\text{S.1})$$

where $\beta = 1/k_B T$, with k_B being the Boltzmann constant and T is the temperature; s is the progression along the MEP and $V_{\text{MEP}}[s_*^{\text{CVT}}(T)]$ is the potential located at $s = s_*^{\text{CVT}}(T)$, that is, the position of the optimal dividing surface perpendicular to the MEP that minimizes the forward flux towards products; $Q^{\text{GT}}[T, s_*^{\text{CVT}}(T)]$ is the partition function calculated at that position of the MEP; and $\Phi_{\text{R}}(T)$ is the partition function of reactants per unit volume and for a unimolecular reaction is replaced by the unitless reactant partition function $Q_{\text{R}}(T)$. The partition functions are separated as the product of translational (trans), rotational (rot), vibrational (vib) and electronic (el) partition functions. For the studied reactions, both the electronic and translational partition functions of the generalized transition state and the reactant cancel out, so the CVT thermal rate constant of Eq. S.1 is rewritten as

$$k^{\text{CVT}}(T) = \frac{1}{h\beta} \frac{Q_{\text{rot}}^{\text{GT}}[T, s_*^{\text{CVT}}(T)] Q_{\text{vib}}^{\text{GT}}[T, s_*^{\text{CVT}}(T)]}{Q_{\text{rot,R}}(T) Q_{\text{vib,R}}(T)} \exp\{-\beta V_{\text{MEP}}[s_*^{\text{CVT}}(T)]\} \quad (\text{S.2})$$

The vibrational partition functions within the harmonic oscillator approximation can be written as

$$Q_{\text{vib}} = \tilde{Q}_{\text{vib}} e^{-\beta \mathcal{E}} \quad (\text{S.3})$$

where

$$\tilde{Q}_{\text{vib}} = \prod_m \frac{1}{1 - e^{-\beta \hbar \omega_m}} \quad (\text{S.4})$$

where \mathcal{E} is the contribution of the zero-point energy (ZPE). In the case of reactants

$$\mathcal{E}_R = \frac{1}{2} \sum_{m=1}^F \hbar \omega_{m,R} \quad (S.5)$$

where $\omega_{m,R}$ are the harmonic normal-mode frequencies of reactants, and the sum runs up to $F = 3N - 6$ (N being the number of atoms). In the case of to the generalized vibrational partition functions the ZPE is given by $F - 1$ modes perpendicular to the reaction coordinate:

$$\mathcal{E}^{GT}(s) = \frac{1}{2} \sum_{m=1}^{F-1} \hbar \omega_m^{GT}(s) \quad (S.6)$$

where $\omega_m^{GT}(s)$ are the generalized normal-mode frequencies. Taking Eqs. S.3, S.5 and S.6 into account, the CVT thermal rate constant of Eq. S.2 can be rewritten as:

$$k^{CVT}(T) = \frac{1}{h\beta} \frac{Q_{rot}^{GT}[T, s_*^{CVT}(T)] \tilde{Q}_{vib}^{GT}[T, s_*^{CVT}(T)]}{Q_{rot,R}(T) \tilde{Q}_{vib,R}(T)} \times \exp \left\{ -\beta (V_{MEP}[s_*^{CVT}(T)] + \mathcal{E}^{GT}[s_*^{CVT}(T)] - \mathcal{E}_R) \right\} \quad (S.7)$$

Quantum effects in all the $F - 1$ degrees of freedom perpendicular to the reaction coordinate are incorporated through the quantum vibrational partition function of Eq. S.3. Quantum effects in the reaction coordinate, mainly tunneling, are incorporated through a multidimensional tunneling (MT) transmission coefficient, $\kappa^{CVT/MT}(T)$ that multiplies the CVT thermal rate constant, i.e.,

$$k^{CVT/MT}(T) = \kappa^{CVT/MT}(T) k^{CVT}(T) \quad (S.8)$$

Tunneling is calculated by adopting the adiabatic separation of the reaction coordinate from the other $F - 1$ degrees of freedom. This approximation assumes that the quantum states in these modes are conserved along the MEP. If we consider that the modes only contribute to the internal energy through their ZPE, the ground-state vibrationally adiabatic potential, $V_a^G(s)$ of Eq. 6 is obtained.

The transmission coefficient obtained with the MT tunneling method is written as a Boltzmann average between the semiclassical adiabatic ground-state (SAG) probability $P^{\text{SAG/MT}}(E)$ and the classical probability, $P_C(E)$,

$$\kappa^{\text{CVT/MT}} = \frac{\int_{E_0}^{\infty} dE \exp(-\beta E) P^{\text{SAG/MT}}(E)}{\int_{V_a^G[s_*^{\text{CVT}}(T)]}^{\infty} dE \exp(-\beta E) P_C(E)} \quad (\text{S.9})$$

The denominator of Eq. S.9 can be easily integrated taking into account that $P_C(E)$ equals zero below $V_a^G[s_*^{\text{CVT}}(T)]$ and is the unity otherwise,

$$\kappa^{\text{CVT/MT}} = \frac{\beta \int_{E_0}^{\infty} dE \exp(-\beta E) P^{\text{SAG/MT}}(E)}{\exp\{-\beta V_a^G[s_*^{\text{CVT}}(T)]\}} \quad (\text{S.10})$$

In Eq. S.9 the lowest energy at which tunneling can occur is E_0 which for a unimolecular reaction leading to one product can be defined as:

$$E_0 = \max \left\{ V_a^G(s = s_R) + \frac{1}{2}\hbar\omega_R^F, V_a^G(s = s_P) + \frac{1}{2}\hbar\omega_P^F \right\} \quad (\text{S.11})$$

where s_R and s_P is the location of reactants and products after following the MEP, and ω_R^F and ω_P^F correspond to the lowest frequency at reactants and products, respectively. The SAG probability is given by

$$P^{\text{SAG/MT}}(E) = \begin{cases} 0, & E < E_0 \\ \{1 + \exp[2\theta^{\text{MT}}(E)]\}^{-1}, & E_0 \leq E \leq V^{\text{AG}} \\ 1 - P^{\text{SAG/MT}}(2V^{\text{AG}} - E), & V^{\text{AG}} \leq E \leq 2V^{\text{AG}} - E_0 \\ 1, & 2V^{\text{AG}} - E_0 < E \end{cases} \quad (\text{S.12})$$

The action integral $\theta^{\text{MT}}(E)$ influences the probability depending on the selected tunneling path. If the tunneling path of the particle at energy E is the same as the MEP, it is assumed that the coupling between the reaction coordinate and the rest of the degrees of freedom is negligible; this is what is called zero-curvature tunneling (ZCT) and

$$\theta^{\text{ZCT}}(E) = h^{-1} \int_{s_0(E)}^{s_1(E)} ds \{2\mu [V_a^G(s) - E]\}^{\frac{1}{2}} \quad (\text{S.13})$$

where $s_0(E)$ and $s_1(E)$ are the left and right classical turning points at which the tunneling energy equals the ground-state vibrationally adiabatic potential.

$$V_a^G(s_0) = V_a^G(s_1) = E \quad (\text{S.14})$$

At very low temperatures the reaction coordinate should be quantized and the continuum of energies of Eq. S.10 should be substituted by a discrete sum over energies. The transmission coefficient calculated, considering the forward reaction in the exothermic direction, becomes

$$\kappa^{\text{CVT/MT}} = \frac{\beta \sum_{n=0}^K \frac{dE_n^R}{dn} P^{\text{SAG/MT}}(E_n^R) \exp(-\beta E_n^R)}{\exp\{-\beta V_a^G [s_*^{\text{CVT}}(T)]\}} + \frac{\beta \int_{V_a^G [s_*^{\text{CVT}}(T)]}^{\infty} dE \exp(-\beta E) P^{\text{SCT}}(E)}{\exp\{-\beta V_a^G [s_*^{\text{CVT}}(T)]\}} \quad (\text{S.15})$$

where K is the maximum value that the quantum number n can reach when exciting the discrete levels of the reaction coordinate motion E_n^R up to V^{AG} , the maximum of the vibrationally adiabatic potential.

Notice that when $T \rightarrow 0$, $V_a^G [s_*^{\text{CVT}}(T)] \rightarrow V^{\text{AG}}$. However, V^{AG} may not coincide with $V_a^{\ddagger G}$, which is the value of the vibrationally ground-state potential at the transition state structure.

The reaction coordinate levels within the harmonic approximation are

$$E_n^R = \left(\frac{1}{2} + n\right) \hbar\omega_F \quad (\text{S.16})$$

where ω_F is the reaction coordinate at reactants after following the MEP.^a The derivative is simply

$$\frac{dE_n^R}{dn} = \hbar\omega_F \quad (\text{S.17})$$

If only the ground state contributes to tunneling Eq. S.15 transforms into

$$\kappa^{\text{CVT/MT}} = \hbar\beta\omega_F P^{\text{SAG/MT}}(E_0) e^{-\beta E_0} e^{\beta V^{\text{AG}}} \quad (\text{S.18})$$

On the other hand, when $T \rightarrow 0$, the partition functions of Eq. S.7 tend to the unity and the exponent

$$\exp\{-\beta (V_{\text{MEP}} [s_*^{\text{CVT}}(T)] + \mathcal{E}^{\text{GT}} [s_*^{\text{CVT}}(T)] - \mathcal{E}_R)\} = \exp\{-\beta (V^{\text{AG}} - \mathcal{E}_R)\} \quad (\text{S.19})$$

The combination of Eqs. S.7, S.18, and S.19 when only the vibrational ground state is populated leads to a temperature independent rate constant

$$k_0^{\text{CVT/MT}} = \frac{\omega_F}{2\pi} P^{\text{MT}}(E_0) = \nu_F P^{\text{MT}}(E_0) \quad (\text{S.20})$$

^aNotice that ω_F is ω_R^F of Eq. S.11.

since the exponents of both expressions cancel out because of Eq. S.19 and that $E_0 = \mathcal{E}_R$.^b

2 Ground-state vibrationally adiabatic potential

The harmonic ground-state vibrationally adiabatic potential of Eq. 6 evaluated at the MPWB1K level was modified in two ways prior to the evaluation of the action integrals. On one hand, the MEP was corrected using the dual-level information. On the other hand, redundant-internal coordinates were employed to project the frequencies along the MEP and anharmonic effects were incorporated into these $F - 1$ modes perpendicular to the reaction coordinate using the so-called ‘quasiharmonic’ approximation, that is, through a frequencies scaling factor.

2.1 Dual-level MEP

The dual-level MEP was built from the MPWB1K information, $V_{\text{MEP}}^{\text{DFT}}(s)$, available along the reaction path but incorporating the F12b-CCSD(T) single-point calculations at the stationary points. The differences between the two levels at the stationary points, taking reactants as reference are:

$$\Delta V^{\ddagger,\text{DL}} = V^{\ddagger,\text{CC}} - V^{\ddagger,\text{DFT}} \quad (\text{S.21})$$

where $V^{\ddagger,\text{CC}}$ and $V^{\ddagger,\text{DFT}}$ are the barrier heights obtained at the coupled-cluster and DFT levels, respectively. Similarly,

$$\Delta\Delta V_r^{\text{DL}} = \Delta V_r^{\text{CC}} - \Delta V_r^{\text{DFT}} \quad (\text{S.22})$$

where ΔV_r^{CC} and ΔV_r^{DFT} are the energies of reaction evaluated at the F12b-CCSD(T)/MPWB1K and MPWB1K levels, respectively.

For energies above reactants, the MEP is corrected by the following linear relation:

$$V_{\text{MEP}}^{\text{DL}}(s) = V_{\text{MEP}}^{\text{DFT}}(s) + \Delta V^{\ddagger,\text{DL}} \left(1 - \frac{s}{s_Y} \right) \quad (\text{S.23})$$

^bIn Eq S.20 we have simplified the nomenclature: $P^{\text{SAG/MT}} \rightarrow P^{\text{MT}}$.

where s_Y is the value of the reaction coordinate at reactants if $s < 0$ and equals $s_1(E = 0)$ if $s > 0$. For energies below reactants the MEP is corrected by:

$$V_{\text{MEP}}^{\text{DL}}(s) = V_{\text{MEP}}^{\text{DFT}}(s) + \Delta\Delta V_r^{\text{DL}} \left(\frac{s - s_1(E = 0)}{s_P - s_1(E = 0)} \right) \quad (\text{S.24})$$

where s_P is the value of the reaction coordinate at products.

Notice that Eq. S.24 only applies if we are interested in the reverse rate constants; this is not the case in this work, so the only modifications on the MEP with respect to the MPWB1K path are due to Eq. S.23. The barrier-height correction of Eq. S.23 is more accurate if the value of $\Delta V^{\ddagger,\text{DL}}$ is small. For the reactions of interest, that is, **R_H** and **R1**, this correction amounts to about 10% or less of the total barrier, since both electronic structure methods yield similar forward barriers. Therefore, it is expected that the dual-level MEP produces more accurate rate constants than the raw MPWB1K level because the adjustment improves the forward barrier heights. At the same time, the modifications are small enough to avoid artificial distortions on the reaction paths.

2.2 Quasiharmonic correction for anharmonicity

As to anharmonic effects, all transition state frequencies were corrected by the SRP scaling factors, $\lambda^{\text{ZPE},\ddagger}$, whereas the ones of the minima were scaled by the recommended factor of $\lambda^{\text{ZPE,M}} = 0.951$. In general, this anharmonic correction is incorporated directly into the partition functions,^{3–6}, and therefore it affects the free energy of activation. In those cases, the ZPE along the MEP is corrected with the same scaling factor as the transition state, that is, $\lambda^{\text{ZPE}}(s) = \lambda^{\text{ZPE},\ddagger}$, even if the point on the path is very close to reactants. Although the variation of the scaling factor with the progression along the path, $\lambda^{\text{ZPE}}(s)$, is not known, we have adopted a linear variation approximation of this factor with the reaction coordinate, which grants a smooth change between the TS and reactants scaling factors. Specifically,

$$\lambda^{\text{ZPE}}(s) = \lambda^{\text{ZPE},\ddagger} + (\lambda^{\text{ZPE,M}} - \lambda^{\text{ZPE},\ddagger}) \frac{s}{s_M} \quad (\text{S.25})$$

where s_M indicates the value of the reaction coordinate at reactants if $s < 0$ or at products if $s > 0$. Therefore, the ground-state vibrationally adiabatic potential employed in the evaluation of the action integrals is given by

$$V_a^G(s) = V_{\text{MEP}}^{\text{DL}}(s) + \lambda^{\text{ZPE}}(s)\mathcal{E}^{\text{GT}}(s) \quad (\text{S.26})$$

where $\lambda^{\text{ZPE}}(s)$ is calculated following Eq. S.25, and $V_{\text{MEP}}^{\text{DL}}(s)$ is given by Eq. S.23.

3 Anharmonicity on the reaction coordinate frequency

All equilibrium structures present low frequency modes associated with the torsional and amine inversion normal modes. This type of motions are depicted in Figure S.1 and listed in Table S.1 for the **st** conformer, which is the reactants structure for all **R_H** and **R1** reactions with the exception of **R1-O** for which $\nu_F^{\text{Anh}}=144.3 \text{ cm}^{-1}$.

Table S.1: Unscaled harmonic-oscillator (HO) normal mode frequencies (in cm^{-1}), ν^{HO} , of the **st** conformer associated with the C-X (τ_{CX} , with X = O, S, Se) and C-N (τ_{CN}) torsional motions and with the NH₂ inversion (inv). The *F* subscript refers to the reaction coordinate frequency at reactants in the HO and anharmonic (Anh) approximations, respectively. The description of each normal mode is also given (main component in bold letters).

X = O			X = S			X = Se		
	Freq.	Description		Freq.	Description		Freq.	Description
ν_F^{HO}	366.4	$\tau_{\text{CN}} + \text{inv}$	196.8	$\tau_{\text{CX}} + \tau_{\text{CN}}$		191.8	inv + τ_{CX}	
ν_F^{Anh}	143.0		150.3			130.3		
ν_1^{HO}	404.2	inv	401.5	$\tau_{\text{CN}} + \text{inv}$		252.4	inv + τ_{CX}	
ν_2^{HO}	560.7	τ_{CX}	421.3	inv		413.1	$\tau_{\text{CN}} + \tau_{\text{CX}}$	

The analysis of the normal modes by the CAMVIB program, a module of the SULISO software package,⁷ showed that torsional and inversion

modes are coupled although there is a main type of motion for each of the modes. Of the three modes listed in Table S.1, ν_F is the reaction coordinate normal mode at reactants that enters Eq. S.20 so we have employed an accurate method to include anharmonicity in this normal mode, whereas ν_1 and ν_2 were treated within the quasiharmonic approximation, as the rest of the transverse modes. Specifically, anharmonicity for ν_F was taken into account by solving the one-dimensional Schrödinger equation using the torsional eigenvalue summation (TES) method.^{8,9} The potential is obtained by scanning the main torsion/inversion motion that corresponds to ν_F but with the rest of degrees of freedom relaxed. The resulting energies are fitted to a Fourier series potential of the type:

$$V(\phi) = \sum_{j=0}^N a_j \cos(j\phi) \quad (\text{S.27})$$

where ϕ is the torsional/inversion angle, N is the number of terms in the expansion, and a_j is a coefficient. The Schrödinger equation to solve is given by:

$$\frac{-\hbar^2}{2} B_\phi \frac{d^2}{d\phi^2} \psi(\phi) + V(\phi) \psi(\phi) = \mathcal{E}_i \psi(\phi) \quad (\text{S.28})$$

where B_ϕ is the Wilson's G matrix element,¹⁰ for the torsional/inversion motion, which in the case of the hindered rotation coincides with the inverse of the reduced moment of inertia of the rotating top. In all cases, B_ϕ was evaluated at the absolute minimum of the potential and considered to be ϕ -independent. The trial wavefunction $\psi(\phi)$ is taken as the solution of the Schrödinger equation for a particle in a ring. Equation S.28 was solved using the procedure detailed in Ref. 9 and implemented in a one-dimensional version of the Q2DTor program.¹¹ The anharmonic frequency ν_F^{Anh} is calculated from the equation

$$\mathcal{E}_{0,F} = \frac{1}{2} \hbar \nu_F^{\text{Anh}} \quad (\text{S.29})$$

where $\mathcal{E}_{0,F}$ is the ground-state energy calculated from Eq. S.28.

Notice that for **st-O**, **st-S**, and **st-Se** the main normal-mode motion of ν_F corresponds to the C-N (not plotted), C-X (Figure S.2) and the inversion (Figure S.3), respectively. However, the three potentials present two minima

associated with the NH₂ inversion, because the torsional motions are coupled with it. Thus, there are two **st-S** structures that are enantiomers and correspond to the two symmetric minima with torsional angles of $\pm 3.9^\circ$ and inversion angles of $\mp 145.5^\circ$, being the barrier between the two structures of a few cm⁻¹. Therefore, the anharmonicity on the reaction coordinate takes into account the effect of having two enantiomers separated by a tiny barrier.

References

- [1] B. C. Garrett and D. G. Truhlar, Criterion of minimum state density in the transition state theory of bimolecular reactions, *J. Chem. Phys.*, 1979, **70**, 1593–1598.
- [2] B. C. Garrett and D. G. Truhlar, Generalized transition state theory. Classical mechanical theory and applications to collinear reactions of hydrogen molecules, *J. Phys. Chem.*, 1979, **83**, 1052–1078.
- [3] J. Zheng, R. Meana-Pañeda and D. G. Truhlar, Prediction of experimentally unavailable product branching ratios for biofuel combustion: The role of anharmonicity in the reaction of isobutanol with OH, *J. Am. Chem. Soc.*, 2014, **136**, 5150–5160.
- [4] L. Gao, J. Zheng, A. Fernández-Ramos, D. G. Truhlar and X. Xu, Kinetics of the methanol reaction with OH at interstellar, atmospheric, and combustion temperatures, *J. Am. Chem. Soc.*, 2018, **140**, 2906–2918.
- [5] J. Wu, L. G. Gao, Z. Varga, X. Xu, W. Ren and D. G. Truhlar, Water catalysis of the reaction of methanol with OH radical in the atmosphere is negligible, *Angew. Chem. Int. Ed.*, 2020, **59**, 10826–10830.
- [6] J. Wu, L. G. Gao, W. Ren and D. G. Truhlar, Anharmonic kinetics of the cyclopentane reaction with hydroxyl radical, *Chem. Sci.*, 2020, **11**, 2511–2523.
- [7] I. H. Williams and P. B. Wilson, SULISO: The Bath suite of vibrational characterization and isotope effect calculation software, *SoftwareX*, 2017, **6**, 1–6.

- [8] B. A. Ellingson, V. A. Lynch, S. L. Mielke and D. G. Truhlar, Statistical thermodynamics of bond torsional modes: Tests of separable, almost-separable, and improved Pitzer–Gwinn approximations, *J. Chem. Phys.*, 2006, **125**, 084305.
- [9] A. Fernández-Ramos, Accurate treatment of two-dimensional non-separable hindered internal rotors, *J. Chem. Phys.*, 2013, **138**, 134112.
- [10] E. B. Wilson, Jr., J. C. Decius and P. C. Cross, *Molecular Vibrations*, Dover Publications, Inc., New York, 1955.
- [11] D. Ferro-Costas, M. N. D. S. Cordeiro, D. G. Truhlar and A. Fernández-Ramos, Q2DTor: A program to treat torsional anharmonicity through coupled pair of torsions in flexible molecules, *Comput. Phys. Commun.*, 2018, **232**, 190–205.

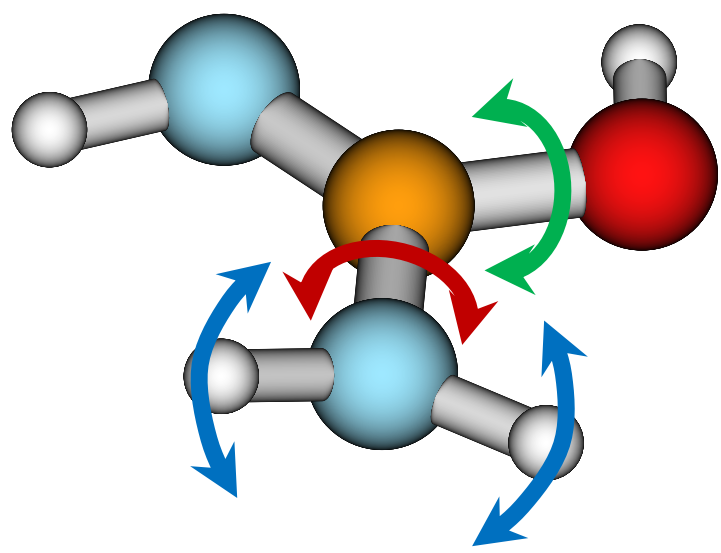


Figure S.1: Depiction of the C-X (green arrow) and C-N (red arrow) torsional modes for the **st** conformer. The inversion motion is indicated by two blue arrows.

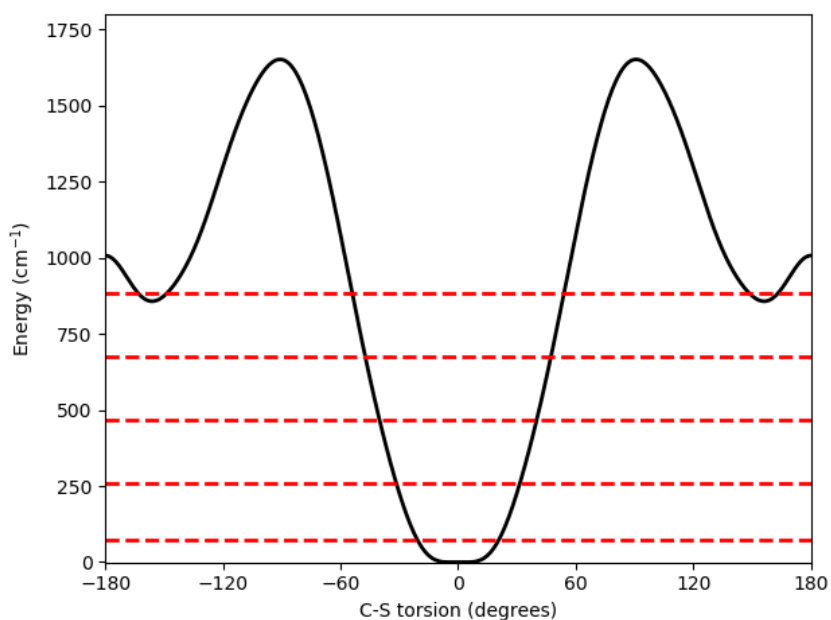


Figure S.2: One-dimensional potential representing the torsion about the C-S single bond. The bottom of the potential corresponds to the **st-S** conformer. The energy levels are indicated by dashed-red lines.

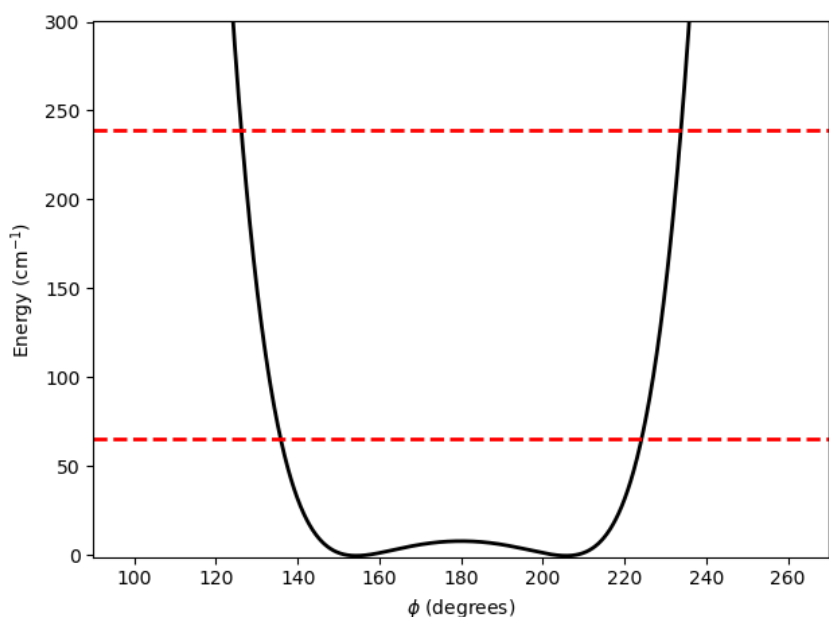


Figure S.3: One-dimensional potential representing the NH_2 inversion of the **st-Se** conformer. The energy levels are indicated by dashed-red lines.

4 Stationary points

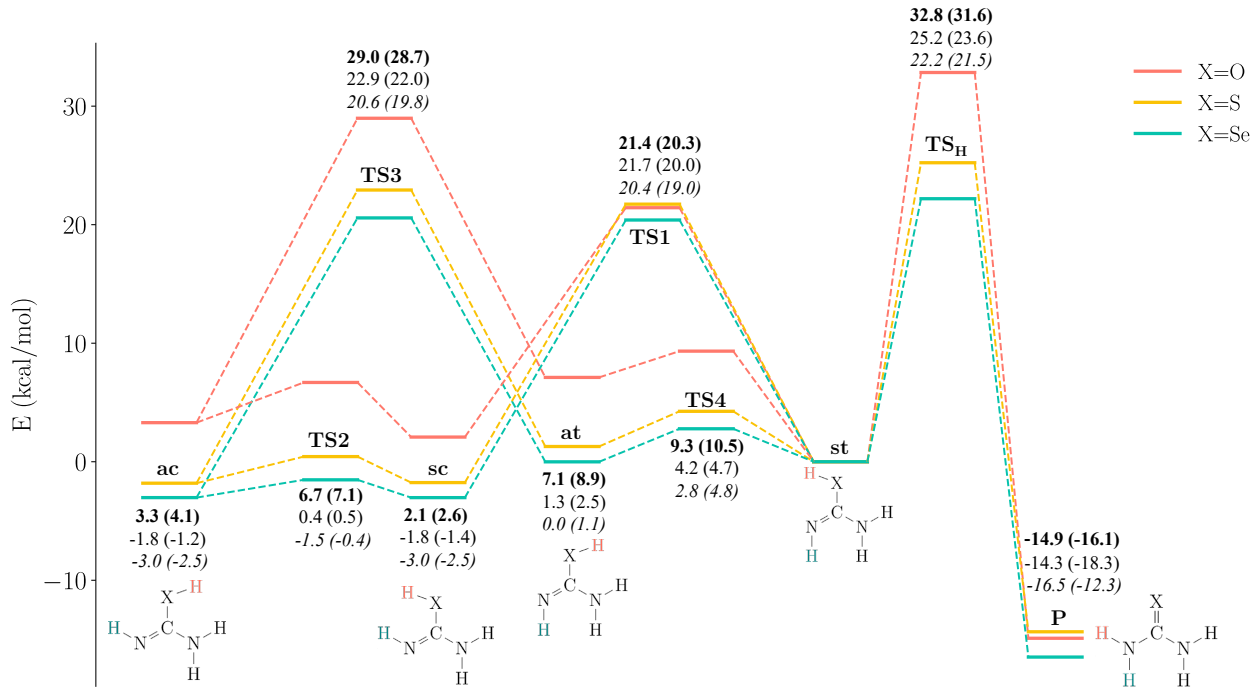


Figure S.4: Schematic representation of the minima participating in the tautomerization reactions. The numbers are the relative electronic energies with respect to the st structures. The energies were obtained at the F12b-CCSD(T)/MPWB1K and MPWB1K (in parentheses) levels. Bold numbers ($X = O$), roman numbers ($X = S$), and italic numbers ($X = Se$).

Table S.2: Geometry, vibrational frequencies and energy for isomer **at-O**. Distances in Å.

Atom	x	y	z	Frequencies (cm ⁻¹)		
N	-0.36	1.22	-0.07	354.95	1127.26	3793.99
C	0.12	-0.07	0.00	411.95	1148.74	3976.48
N	1.31	-0.48	0.00	516.84	1263.78	
O	-0.87	-0.98	0.04	586.61	1475.09	
H	-1.13	1.43	0.54	609.83	1684.92	
H	0.35	1.94	-0.05	738.62	1857.82	
H	-1.65	-0.62	-0.38	845.26	3663.80	
H	1.96	0.30	0.06	1002.75	3674.44	
Method	Energy (Hartree)					
MPWB1K	225.139578					
CCSD(T)-F12	-224.999779					

Table S.3: Geometry, vibrational frequencies and energy for isomer **sc-O**. Distances in Å.

Atom	x	y	z	Frequencies (cm ⁻¹)		
N	1.30	-0.08	-0.06	300.00	1123.97	3865.26
C	-0.05	-0.10	-0.00	396.43	1141.60	4002.49
N	-0.71	-1.17	0.01	490.51	1248.32	
O	-0.52	1.17	0.00	529.11	1505.20	
H	1.77	0.76	0.23	572.56	1664.28	
H	1.76	-0.95	0.12	744.14	1840.42	
H	-1.48	1.16	0.03	772.33	3668.63	
H	-1.71	-1.02	-0.01	1001.67	3728.58	
Method	Energy (Hartree)					
MPWB1K	-225.149678					
CCSD(T)-F12	-225.007798					

Table S.4: Geometry, vibrational frequencies and energy for isomer **ac-O**. Distances in Å.

Atom	x	y	z	Frequencies (cm ⁻¹)		
N	1.25	-0.34	-0.08	379.61	1137.83	3788.70
C	-0.10	-0.08	0.00	431.42	1186.24	3959.18
N	-0.96	-1.00	0.02	509.46	1249.32	
O	-0.40	1.23	0.04	553.80	1479.78	
H	1.83	0.19	0.56	636.07	1674.82	
H	1.45	-1.32	-0.05	786.39	1867.55	
H	0.31	1.74	-0.36	869.67	3665.59	
H	-1.89	-0.60	-0.04	988.82	3671.59	
Method	Energy (Hartree)					
MPWB1K	-225.147310					
CCSD(T)-F12	-225.005861					

Table S.5: Geometry, vibrational frequencies and energy for isomer **st-O**. Distances in Å.

Atom	x	y	z	Frequencies (cm ⁻¹)		
N	-1.30	-0.08	-0.06	366.36	1111.61	3855.47
C	0.05	0.09	0.00	403.24	1135.85	3949.54
N	0.74	1.15	0.00	504.63	1289.13	
O	0.67	-1.10	0.00	560.72	1526.61	
H	-1.65	-0.99	0.16	567.83	1680.01	
H	-1.87	0.70	0.19	763.80	1834.34	
H	1.61	-0.91	0.00	786.43	3679.21	
H	0.17	1.98	-0.01	1017.63	3721.79	
Method	Energy (Hartree)					
MPWB1K	-225.153786					
CCSD(T)-F12	-225.011115					

Table S.6: Geometry, vibrational frequencies and energy for **P-O**. Distances in Å.

Atom	x	y	z	Frequencies (cm ⁻¹)		
N	0.00	1.15	-0.60	366.97	1069.16	3835.46
C	0.00	0.00	0.14	443.28	1201.72	3835.80
N	0.00	-1.15	-0.60	481.37	1477.26	
O	0.00	0.00	1.35	536.09	1669.22	
H	0.18	1.98	-0.07	548.11	1678.28	
H	0.39	1.14	-1.52	588.87	1884.49	
H	-0.18	-1.98	-0.07	803.85	3703.23	
H	-0.40	-1.14	-1.52	1005.04	3708.08	
Method	Energy (Hartree)					
MPWB1K	-225.179433					
CCSD(T)-F12	-225.034849					

Table S.7: Geometry, vibrational frequencies and energy for **TS_H-O**. Distances in Å.

Atom	x	y	z	Frequencies (cm ⁻¹)		
N	-1.09	-1.08	0.14	-1982.30	1106.17	3746.44
C	-0.41	0.06	0.04	104.66	1151.59	3882.54
N	-0.82	1.30	-0.03	292.93	1178.75	
O	0.87	0.10	0.02	465.35	1616.11	
H	-0.58	-1.94	0.12	533.97	1684.28	
H	-2.08	-1.11	0.07	697.81	1731.85	
H	0.48	1.32	-0.04	787.36	2304.60	
H	-1.78	1.61	0.00	1078.12	3741.05	
Method	Energy (Hartree)					
MPWB1K	-225.103477					
CCSD(T)-F12	-224.958782					

Table S.8: Geometry, vibrational frequencies and energy for **TS1-O**. Distances in Å.

Atom	x	y	z	Frequencies (cm ⁻¹)		
N	1.34	-0.04	0.03	-931.04	1008.23	3920.17
C	0.00	-0.08	-0.06	314.30	1107.71	3962.42
N	-0.72	-1.11	-0.11	491.70	1257.65	
O	-0.49	1.17	0.03	528.31	1445.85	
H	1.80	0.81	0.29	531.78	1652.14	
H	1.82	-0.91	0.09	584.12	1834.44	
H	-1.45	1.08	0.00	631.76	3725.98	
H	-1.11	-1.66	-0.84	782.82	3878.20	
Method	Energy (Hartree)					
MPWB1K	-225.121419					
CCSD(T)-F12	-224.976962					

Table S.9: Geometry, vibrational frequencies and energy for **TS2-O**. Distances in Å.

Atom	x	y	z	Frequencies (cm ⁻¹)		
N	1.33	-0.09	-0.07	-402.69	1137.24	3842.97
C	-0.03	-0.10	-0.03	449.25	1167.79	3981.66
N	-0.70	-1.17	0.01	518.21	1213.31	
O	-0.56	1.16	-0.01	543.08	1458.39	
H	1.77	0.74	0.27	566.36	1662.37	
H	1.78	-0.96	0.13	699.55	1842.51	
H	-0.74	1.45	-0.91	842.08	3674.30	
H	-1.69	-0.96	0.00	978.13	3710.02	
Method				Energy (Hartree)		
MPWB1K				-225.142379		
CCSD(T)-F12				-225.000456		

Table S.10: Geometry, vibrational frequencies and energy for **TS3-O**. Distances in Å.

Atom	x	y	z	Frequencies (cm ⁻¹)		
N	0.80	-1.01	-0.07	-1016.51	971.36	3967.92
C	-0.14	0.01	0.00	102.98	1104.25	4076.50
N	-1.35	-0.11	0.02	379.25	1260.41	
O	0.46	1.23	0.03	412.83	1362.39	
H	1.63	-0.90	0.48	533.01	1678.26	
H	0.38	-1.92	0.02	599.81	1976.13	
H	1.36	1.16	-0.30	625.14	3676.95	
H	-2.32	-0.26	0.00	759.21	3802.66	
Method				Energy (Hartree)		
MPWB1K				-225.107955		
CCSD(T)-F12				-224.964934		

Table S.11: Geometry, vibrational frequencies and energy for **TS4-O**. Distances in Å.

Atom	x	y	z	Frequencies (cm ⁻¹)		
N	-0.29	1.18	0.33	-419.09	1119.22	3823.11
C	0.19	-0.09	0.09	458.78	1151.94	3981.35
N	1.36	-0.47	-0.11	507.19	1226.91	
O	-0.83	-0.99	0.10	538.28	1451.57	
H	-1.24	1.35	0.07	594.91	1675.02	
H	0.34	1.94	0.15	687.22	1840.74	
H	-1.09	-1.18	1.00	869.16	3642.43	
H	2.00	0.31	-0.16	997.83	3696.88	
Method				Energy (Hartree)		
MPWB1K				-225.137041		
CCSD(T)-F12				-224.996245		

Table S.12: Geometry, vibrational frequencies and energy for isomer **at-S**. Distances in Å.

Atom	x	y	z	Frequencies (cm ⁻¹)		
N	-1.09	1.11	0.05	197.95	966.89	3677.82
C	-0.47	-0.12	0.00	362.18	1114.32	3801.87
N	-1.00	-1.26	0.02	390.04	1138.41	
S	1.30	-0.07	-0.03	466.43	1386.67	
H	-0.64	1.86	-0.43	523.12	1675.46	
H	-2.08	1.10	-0.06	618.18	1788.84	
H	1.42	1.14	0.52	711.14	2795.84	
H	-2.01	-1.21	-0.04	847.84	3608.76	
Method				Energy (Hartree)		
MPWB1K				-548.161486		
CCSD(T)-F12				-547.593218		

Table S.13: Geometry, vibrational frequencies and energy for isomer **sc-S**. Distances in Å.

Atom	x	y	z	Frequencies (cm ⁻¹)		
N	-1.15	-1.06	-0.04	213.59	952.01	3690.34
C	-0.49	0.13	0.00	367.20	1130.16	3824.23
N	-1.10	1.23	0.00	416.91	1167.86	
S	1.28	-0.14	-0.04	467.93	1381.45	
H	-0.74	-1.85	0.42	521.74	1659.61	
H	-2.15	-0.98	0.02	652.45	1792.76	
H	1.59	1.03	0.51	697.93	2820.15	
H	-0.49	2.02	-0.09	809.37	3683.81	
Method				Energy (Hartree)		
MPWB1K				-548.167709		
CCSD(T)-F12				-547.598070		

Table S.14: Geometry, vibrational frequencies and energy for isomer **ac-S**. Distances in Å.

Atom	x	y	z	Frequencies (cm ⁻¹)		
N	1.12	-1.09	0.05	224.52	936.79	3675.02
C	0.49	0.12	0.00	367.32	1136.08	3806.53
N	1.13	1.20	0.01	421.09	1174.07	
S	-1.29	0.02	-0.04	461.94	1388.76	
H	0.71	-1.84	-0.47	557.84	1658.83	
H	2.12	-1.01	-0.03	664.21	1794.29	
H	-1.39	-1.06	0.72	698.62	2797.51	
H	0.53	2.01	0.10	848.52	3673.63	
Method				Energy (Hartree)		
MPWB1K				-548.167415		
CCSD(T)-F12				-547.598152		

Table S.15: Geometry, vibrational frequencies and energy for isomer **st-S**. Distances in Å.

Atom	x	y	z	Frequencies (cm ⁻¹)		
N	-1.15	-1.06	-0.06	196.81	930.34	3697.35
C	-0.46	0.12	0.00	364.42	1114.89	3822.94
N	-0.93	1.30	0.00	401.49	1139.75	
S	1.29	-0.12	-0.01	421.33	1391.62	
H	-0.69	-1.89	0.26	476.77	1683.98	
H	-2.13	-1.02	0.12	622.84	1783.76	
H	1.54	1.18	0.13	709.84	2831.50	
H	-1.94	1.30	0.01	820.42	3607.30	
Method				Energy (Hartree)		
MPWB1K				-548.165456		
CCSD(T)-F12				-547.595267		

Table S.16: Geometry, vibrational frequencies and energy for **P-S**. Distances in Å.

Atom	x	y	z	Frequencies (cm ⁻¹)		
N	1.04	-1.14	0.04	262.80	1077.79	3841.59
C	0.31	0.00	0.00	358.73	1101.34	3842.28
N	1.04	1.14	-0.04	408.94	1461.86	
S	-1.34	0.00	0.00	467.90	1494.41	
H	0.53	-1.99	-0.04	473.59	1675.94	
H	2.00	-1.15	-0.22	596.81	1695.65	
H	0.53	1.99	0.04	653.21	3694.97	
H	2.00	1.15	0.22	799.66	3702.56	
Method				Energy (Hartree)		
MPWB1K				-548.194638		
CCSD(T)-F12				-547.618128		

Table S.17: Geometry, vibrational frequencies and energy for **TS_H-S**. Distances in Å.

Atom	x	y	z	Frequencies (cm ⁻¹)		
N	-1.16	-1.08	0.10	-1727.79	848.64	3730.51
C	-0.44	0.04	0.04	188.86	1090.06	3867.81
N	-0.86	1.26	-0.02	389.72	1201.38	
S	1.29	0.11	0.02	444.92	1442.77	
H	-0.71	-1.97	0.13	507.95	1650.59	
H	-2.16	-1.06	0.11	634.69	1714.04	
H	0.50	1.50	-0.04	676.96	1903.66	
H	-1.85	1.48	-0.02	749.78	3627.74	
Method				Energy (Hartree)		
MPWB1K				-548.127839		
CCSD(T)-F12				-547.555067		

Table S.18: Geometry, vibrational frequencies and energy for **TS1-S**. Distances in Å.

Atom	x	y	z	Frequencies (cm ⁻¹)		
N	-1.15	-1.11	0.00	-992.28	669.77	3837.53
C	-0.49	0.08	-0.04	217.52	915.24	3990.01
N	-0.99	1.20	-0.18	295.98	1141.95	
S	1.28	-0.21	0.23	369.23	1288.44	
H	-0.73	-1.91	0.43	420.08	1663.51	
H	-2.15	-1.06	-0.02	457.67	1874.02	
H	1.56	1.08	0.30	506.79	2840.54	
H	-1.34	1.91	-0.77	658.95	3696.73	
Method				Energy (Hartree)		
MPWB1K				-548.133600		
CCSD(T)-F12				-547.560636		

Table S.19: Geometry, vibrational frequencies and energy for **TS2-S**. Distances in Å.

Atom	x	y	z	Frequencies (cm ⁻¹)		
N	-1.10	1.03	-0.22	-211.48	944.31	3712.62
C	-0.45	-0.14	-0.04	273.74	1141.26	3866.75
N	-1.06	-1.23	0.12	381.53	1155.73	
S	1.36	0.05	-0.09	456.88	1378.05	
H	-0.60	1.90	-0.18	479.28	1651.03	
H	-2.09	1.04	-0.04	593.88	1799.09	
H	1.46	-0.33	-1.37	683.26	2802.48	
H	-0.42	-2.00	0.24	841.64	3689.95	
Method				Energy (Hartree)		
MPWB1K				-548.164670		
CCSD(T)-F12				-547.594576		

Table S.20: Geometry, vibrational frequencies and energy for **TS3-S**. Distances in Å. ok

Atom	x	y	z	Frequencies (cm ⁻¹)		
N	-1.07	1.11	-0.06	-1005.30	668.91	3820.47
C	-0.43	-0.09	-0.28	180.49	907.64	4030.82
N	-0.97	-1.17	-0.48	277.36	1143.51	
S	1.37	0.04	-0.27	378.66	1283.21	
H	-0.61	1.96	-0.33	417.82	1664.59	
H	-2.06	1.08	-0.22	457.70	1902.80	
H	1.49	1.29	0.18	518.39	2783.31	
H	-1.43	-2.02	-0.31	660.62	3686.93	
Method				Energy (Hartree)		
MPWB1K				-548.130458		
CCSD(T)-F12				-547.558735		

Table S.21: Geometry, vibrational frequencies and energy for **TS4-S**. Distances in Å.

Atom	x	y	z	Frequencies (cm ⁻¹)		
N	-1.11	1.08	-0.02	-240.53	965.70	3695.80
C	-0.48	-0.13	0.00	361.25	1108.69	3836.30
N	-1.00	-1.28	0.08	397.09	1146.07	
S	1.31	0.01	-0.07	449.16	1374.08	
H	-0.58	1.88	-0.30	472.51	1664.64	
H	-2.10	1.11	-0.17	563.00	1790.97	
H	1.45	0.11	1.25	696.32	2802.25	
H	-2.02	-1.22	0.10	879.99	3576.09	
Method	Energy (Hartree)					
MPWB1K	-548.157908					
CCSD(T)-F12	-547.588486					

Table S.22: Geometry, vibrational frequencies and energy for isomer **at-Se**. Distances in Å.

Atom	x	y	z	Frequencies (cm ⁻¹)		
C	0.94	-0.12	-0.01	214.30	879.78	3687.49
Se	-0.94	-0.03	0.01	336.71	1106.72	3818.03
N	1.60	1.08	-0.05	363.86	1137.50	
N	1.45	-1.27	-0.01	386.99	1376.31	
H	1.14	1.89	0.31	430.43	1681.90	
H	2.59	1.05	0.11	609.57	1777.18	
H	-1.03	1.39	-0.27	654.90	2549.79	
H	2.46	-1.24	0.02	838.19	3605.96	
Method	Energy (Hartree)					
MPWB1K	-2549.625831					
CCSD(T)-F12	-521.886773					

Table S.23: Geometry, vibrational frequencies and energy for isomer **sc-Se**. Distances in Å.

Atom	x	y	z	Frequencies (cm ⁻¹)		
C	-0.96	0.13	0.00	206.69	859.10	3688.08
Se	0.94	-0.05	-0.02	317.04	1131.76	3820.70
N	-1.57	-1.09	-0.04	376.70	1164.98	
N	-1.64	1.19	0.00	387.79	1375.71	
H	-1.12	-1.87	0.40	503.64	1663.49	
H	-2.57	-1.05	0.03	642.82	1786.52	
H	1.17	1.30	0.43	660.73	2574.68	
H	-1.08	2.02	-0.08	817.48	3685.00	
Method	Energy (Hartree)					
MPWB1K	-2549.631607					
CCSD(T)-F12	-521.891586					

Table S.24: Geometry, vibrational frequencies and energy for isomer **ac-Se**. Distances in Å.

Atom	x	y	z	Frequencies (cm ⁻¹)		
C	0.96	0.12	0.01	199.62	852.61	3676.97
Se	-0.94	0.02	-0.01	322.88	1137.97	3814.67
N	1.60	-1.08	0.05	376.11	1168.98	
N	1.61	1.20	0.00	399.76	1386.72	
H	1.17	-1.86	-0.42	527.62	1659.83	
H	2.60	-1.01	-0.07	650.03	1782.05	
H	-1.02	-1.33	0.49	663.37	2552.92	
H	1.02	2.01	0.09	831.13	3670.65	
Method	Energy (Hartree)					
MPWB1K	2549.631615					
CCSD(T)-F12	-521.891583					

Table S.25: Geometry, vibrational frequencies and energy for isomer **st-Se**. Distances in Å.

Atom	x	y	z	Frequencies (cm ⁻¹)		
C	-0.94	0.12	0.00	191.83	834.73	3705.62
Se	0.94	-0.06	0.00	252.40	1105.00	3837.19
N	-1.58	-1.08	-0.05	317.84	1138.80	
N	-1.46	1.27	0.00	399.84	1375.45	
H	-1.09	-1.92	0.15	413.05	1689.96	
H	-2.57	-1.10	0.13	609.12	1773.99	
H	1.12	1.38	0.06	649.81	2599.74	
H	-2.48	1.23	0.00	822.92	3595.06	
Method				Energy (Hartree)		
MPWB1K				-2549.627561		
CCSD(T)-F12				-521.886761		

Table S.26: Geometry, vibrational frequencies and energy for **P-Se**. Distances in Å.

Atom	x	y	z	Frequencies (cm ⁻¹)		
N	1.45	-1.14	0.04	239.21	1087.47	3838.03
C	0.73	0.00	0.00	347.60	1130.84	3839.30
N	1.45	1.14	-0.04	368.16	1480.11	
Se	-0.92	0.00	0.00	440.07	1568.64	
H	0.94	-1.99	-0.04	496.42	1675.84	
H	2.42	-1.15	-0.22	605.70	1711.88	
H	0.94	1.99	0.04	632.83	3690.78	
H	2.42	1.15	0.22	822.11	3698.68	
Method				Energy (Hartree)		
MPWB1K				-2549.647210		
CCSD(T)-F12				-521.913023		

Table S.27: Geometry, vibrational frequencies and energy for **TS_H-Se**. Distances in Å.

Atom	x	y	z	Frequencies (cm ⁻¹)		
N	-1.21	-1.11	0.16	-1633.44	866.95	3725.13
C	-0.45	-0.04	-0.12	292.83	1089.55	3863.71
N	-0.85	1.18	-0.26	333.95	1205.54	
Se	1.39	-0.03	-0.36	483.01	1429.88	
H	-0.79	-2.01	0.25	534.34	1653.39	
H	-2.20	-1.03	0.27	544.47	1706.73	
H	0.55	1.43	-0.48	662.96	1813.12	
H	-1.83	1.41	-0.17	719.31	3605.92	
Method	Energy (Hartree)					
MPWB1K	-2549.593268					
CCSD(T)-F12	-521.851398					

Table S.28: Geometry, vibrational frequencies and energy for **TS1-Se**. Distances in Å.

Atom	x	y	z	Frequencies (cm ⁻¹)		
N	-1.54	-1.08	-0.01	-980.42	667.38	3843.75
C	-0.91	0.11	-0.11	216.80	829.20	3999.85
N	-1.45	1.21	-0.23	259.83	1141.92	
Se	1.01	-0.15	0.06	316.85	1279.12	
H	-1.06	-1.90	0.32	333.95	1669.17	
H	-2.54	-1.08	0.02	365.55	1884.37	
H	1.25	1.28	0.05	511.40	2602.69	
H	-1.88	1.92	-0.77	633.46	3697.84	
Method	Energy (Hartree)					
MPWB1K	-2549.597260					
CCSD(T)-F12	-521.854260					

Table S.29: Geometry, vibrational frequencies and energy for **TS2-Se**. Distances in Å.

Atom	x	y	z	Frequencies (cm ⁻¹)		
N	-1.58	-1.05	0.05	-180.59	878.65	3717.25
C	-0.91	0.12	0.01	216.09	1135.79	3878.95
N	-1.51	1.23	0.01	328.72	1160.60	
Se	1.00	-0.10	-0.02	373.73	1377.24	
H	-1.09	-1.92	0.08	485.53	1648.13	
H	-2.58	-1.02	0.12	596.63	1791.14	
H	1.07	-0.02	-1.46	634.22	2540.49	
H	-0.87	2.01	0.00	842.48	3689.18	
Method	Energy (Hartree)					
MPWB1K	-2549.628216					
CCSD(T)-F12	-521.889193					

Table S.30: Geometry, vibrational frequencies and energy for **TS3-Se**. Distances in Å.

Atom	x	y	z	Frequencies (cm ⁻¹)		
N	-1.60	-1.12	-0.05	-985.37	660.44	3840.45
C	-0.92	0.06	-0.13	201.87	816.36	4014.37
N	-1.43	1.17	-0.24	280.33	1142.70	
Se	0.99	-0.11	0.02	326.70	1280.14	
H	-1.16	-1.93	0.35	367.10	1665.20	
H	-2.59	-1.06	0.03	380.86	1885.88	
H	1.08	-1.56	0.02	477.32	2530.55	
H	-1.85	1.93	-0.71	634.91	3696.16	
Method	Energy (Hartree)					
MPWB1K	-2549.596030					
CCSD(T)-F12	-521.853979					

Table S.31: Geometry, vibrational frequencies and energy for **TS4-Se**. Distances in Å.

Atom	x	y	z	Frequencies (cm ⁻¹)		
N	-1.60	-1.07	0.03	-221.98	882.46	3704.84
C	-0.95	0.12	0.00	226.57	1099.70	3853.32
N	-1.46	1.28	-0.02	336.38	1150.17	
Se	0.95	-0.06	-0.01	388.23	1363.91	
H	-1.08	-1.92	0.11	484.76	1663.80	
H	-2.60	-1.11	0.13	550.98	1780.46	
H	1.03	-0.10	-1.45	638.96	2543.78	
H	-2.48	1.23	0.00	866.25	3566.84	
Method	Energy (Hartree)					
MPWB1K	-2549.619925					
CCSD(T)-F12	-521.882327					